


# Value of Fluid-Attenuated Inversion Recovery MRI Data Analyzed by the Lesion Segmentation Toolbox in Amyotrophic Lateral Sclerosis

Anna M. Wirth, MS,<sup>1,2</sup> Siw Johannesen, MD,<sup>1</sup> Andrei Khomenko, MD,<sup>1</sup> Dobri Baldaranov, MD,<sup>1</sup> Tim-Henrik Bruun, PhD,<sup>1</sup> Christina Wendl, MD,<sup>3</sup> Gerhard Schuierer, MD,<sup>3</sup> Mark W. Greenlee, PhD,<sup>2</sup> and Ulrich Bogdahn, MD<sup>1†\*</sup> 

**Background:** MRI fluid-attenuated inversion recovery (FLAIR) studies reported hyperintensity in the corticospinal tract and corpus callosum of patients with amyotrophic lateral sclerosis (ALS).

**Purpose:** To evaluate the lesion segmentation toolbox (LST) for the objective quantification of FLAIR lesions in ALS patients.

**Study Type:** Retrospective.

**Population:** Twenty-eight ALS patients (eight females, mean age: 50 range: 24–73, mean ALSFRS-R sum score: 36) were compared with 31 age-matched healthy controls (12 females, mean age: 45, range: 25–67). ALS patients were treated with riluzole and additional G-CSF (granulocyte-colony stimulating factor) on a named patient basis.

**Field Strength/Sequence:** 1.5 T, FLAIR, T<sub>1</sub>-weighted MRI.

**Assessment:** The lesion prediction algorithm (LPA) of the LST enabled the extraction of individual binary lesion maps, total lesion volume (TLV), and number (TLN). Location and overlap of FLAIR lesions across patients were investigated by registration to FLAIR average space and an atlas. ALS-specific functional rating scale revised (ALSFRS-R), disease progression, and survival since diagnosis served as clinical correlates.

**Statistical Tests:** Univariate analysis of variance (ANOVA), repeated-measures ANOVA, t-test, Bravais-Pearson correlation, Chi-square test of independence, Kaplan–Meier analysis, Cox-regression analysis.

**Results:** Both ALS patients and healthy controls exhibited FLAIR alterations. TLN significantly depended on age ( $F(1,54) = 24.659, P < 0.001$ ) and sex ( $F(1,54) = 5.720, P = 0.020$ ). ALS patients showed higher TLN than healthy controls depending on sex ( $F(1, 54) = 5.076, P = 0.028$ ). FLAIR lesions were small and most pronounced in male ALS patients. FLAIR alterations were predominantly detected in the superior and posterior corona radiata, anterior capsula interna, and posterior thalamic radiation. Patients with pyramidal tract (PT) lesions exhibited significantly inferior survival than patients without PT lesions ( $P = 0.013$ ). Covariate age exhibited strong prognostic value for survival ( $P = 0.015$ ).

**Data Conclusion:** LST enables the objective quantification of FLAIR alterations and is a potential prognostic biomarker for ALS.

**Level of Evidence:** 3

**Technical Efficacy:** Stage 2

J. MAGN. RESON. IMAGING 2019;50:552–559.

**A**MYOTROPHIC LATERAL SCLEROSIS (ALS) is a progressive neurodegenerative disease involving both upper motor neurons (UMN) and lower motor neurons (LMN) as well as nonmotor areas like the frontotemporal cortex.<sup>1</sup> The diagnostic process for this disorder is delayed by the great clinical heterogeneity of ALS phenotypes due to

View this article online at [wileyonlinelibrary.com](http://wileyonlinelibrary.com). DOI: 10.1002/jmri.26577

Received Sep 14, 2018, Accepted for publication Oct 29, 2018.

\*Address reprint requests to: U.B., Department of Neurology, University Hospital of Regensburg, Universitätsstraße 84, 93053, Regensburg, Germany.

E-mail: [uli.bogdahn@ukr.de](mailto:uli.bogdahn@ukr.de)

<sup>†</sup>U. Bogdahn is the senior author.

Contract grant sponsor: German Federal Ministry of Education and Research; BMBF, Project GO-Bio.

From the <sup>1</sup>Department of Neurology, University Hospital of Regensburg, Germany; <sup>2</sup>Department of Experimental Psychology, University of Regensburg, Germany; and <sup>3</sup>Center of Neuroradiology, University Hospital and District Medical Hospital of Regensburg, Germany

This is an open access article under the terms of the Creative Commons Attribution-NonCommercial License, which permits use, distribution and reproduction in any medium, provided the original work is properly cited and is not used for commercial purposes.

variability of onset (limb or bulbar), extent of UMN and LMN involvement, and affected site (upper or lower limbs, distal or proximal muscles). Facing the psychological impact of a life-threatening diagnosis, precise ALS diagnosis requires the reliable exclusion of other disorders.<sup>2</sup> Electromyography, lumbar puncture, and magnetic resonance imaging (MRI) may provide promising biomarkers, improving the classification of ALS and the identification of mimic disorders.<sup>1,2</sup>

MRI findings like cortical thinning of the precentral cortex as well as reduced fractional anisotropy of the corticospinal tract (CST) and corpus callosum (CC) are promising biomarkers for ALS.<sup>3</sup> CST involvement in ALS may be detected by brain MRI as well as spinal cord MRI.<sup>4</sup> Conventional fluid-attenuated inversion recovery (FLAIR) imaging is a T<sub>2</sub>-weighted MRI sequence that eliminates signals derived from free cerebrospinal fluid.<sup>5</sup> FLAIR imaging enables the detection of cortical, subcortical, and paraventricular lesions and is considered a crucial sequence for multiple sclerosis (MS).<sup>6,7</sup> In ALS, FLAIR imaging studies could show a pathological signal increase in the CST<sup>8–12</sup> and the CC.<sup>12</sup> However, the sensitivity and specificity of FLAIR imaging for ALS are controversial, as FLAIR hyperintensity is also detectable in healthy controls<sup>13,14</sup> and was predominantly found in ALS patients with disease progression.<sup>15</sup> Only a few studies using FLAIR imaging objectively quantified FLAIR alterations in ALS.<sup>8,10,12,16</sup> The automated lesion segmentation toolbox (LST) established in MS research enables the objective and time-saving quantification of white matter (WM) lesions in FLAIR images.<sup>17</sup>

Thus, the aim of this study was to evaluate the potential of the LST in the detection of FLAIR lesions in ALS patients. We investigated the localization and overlap of FLAIR lesions across patients and potential correlations to clinical data.

## Materials and Methods

### Participants

The unicenter project was carried out in accordance with the Declaration of Helsinki<sup>18</sup> and was approved by the local Ethics Committee (ethics approval: 15-101-0106). Written informed consent was obtained prior to participation. The sample of this study was composed of 28 ALS patients compared with 31 age-matched healthy controls. Overall, 25 patients were diagnosed with classic limb-onset ALS, whereas another three patients exhibited bulbar-onset of the disease. All ALS patients received riluzole standard therapy and additional G-CSF (granulocyte-colony stimulating factor, Filgrastim) on a named patient basis. Application modes and doses of G-CSF were individually adapted; treatment duration was up to 7 years. Safety and monitoring of ALS patients required the assessment of ALSFRS-R scores every month and MRI acquisition every 3 months.

### Data Acquisition

Structural FLAIR MRI was performed on two 1.5 T clinical scanners using identical settings (Aera, Sonata, Siemens Medical, Erlangen, Germany) with 2D-axial orientation (repetition time

[TR] = 7530 msec, echo time [TE] = 110 msec, inversion time [TI] = 2300 msec, flip angle [FA]: 180°, 21 slices, slice thickness: 5 mm, gap: 0.2, number of averages: 1, matrix: 256 × 196). A FLAIR average template (resolution: 2 mm,  $n = 853$  subjects)<sup>19</sup> served as a reference for the transfer of regions of interest (ROIs) (see section Locations and Overlap of FLAIR Lesions). T<sub>1</sub>-weighted structural images were assessed in all healthy controls and a subset of ALS patients ( $n = 20$ ) using a magnetization prepared rapid gradient echo sequence (MPRAGE) (TR: 2220 msec, TE: 5.97 msec, FA: 15°, voxel size: 1 × 1 × 1 mm<sup>3</sup>, field of view [FOV]: 256 × 256 mm<sup>2</sup>, 176 sagittal slices covering the whole brain).

### Lesion Segmentation Toolbox

Individual FLAIR data were analyzed by the lesion prediction algorithm (LPA)<sup>20</sup> included in the freeware LST v. 2.0.15 ([www.statistical-modelling.de/lst.html](http://www.statistical-modelling.de/lst.html)) for SPM (SPM12, MatLab v. 2015b; MathWorks, Natick, MA). LPA involves a binary classifier based on the logistic regression model developed on data from 53 patients with severe MS lesions.<sup>20</sup> The model involves lesion belief maps and considers spatial covariates. Based on the model, lesions are segmented by calculation of lesion probabilities for each voxel. Raw FLAIR data were preprocessed and lesion probability maps were estimated. Values of interest like TLV (total lesion volume in ml) and TLN (number of lesions) were extracted by thresholding individual lesion probability maps. Threshold kappa was set to  $\kappa = 0.5$ , as this threshold was recommended for LPA SPM12 use.<sup>21</sup> Binary lesion maps thresholded by  $\kappa$  enabled the visualization of individual patients' FLAIR lesions. T<sub>1</sub> data are not required for LPA use. However, LPA provides the possibility for T<sub>1</sub> registration in the case of low-resolution FLAIR images.<sup>20</sup> A separate control analysis involving all healthy controls and a subset of ALS patients ( $n = 20$ ) investigated effects of precedent T<sub>1</sub> registration on LPA results.

### Locations and Overlap of FLAIR Lesions

Individual FLAIR images of ALS patients were registered to the FLAIR average template<sup>19</sup> by linear and nonlinear registration tools (FLIRT, FNIRT) of FSL (Freesurfer v. 3.2). Individual binary lesion maps were transferred to an average FLAIR template. Localization of FLAIR lesions was performed by the use of a WM atlas.<sup>22</sup> The atlas defines 48 WM areas in average diffusion-weighted imaging (DWI) space. Masks of these WM regions were registered from average DWI space to average FLAIR space by FLIRT and enabled the description of locations of FLAIR lesions. Addition of individual binary lesion maps across ALS patients enabled the investigation of size and distribution of FLAIR lesions across individual ALS patients.

### Quantitative and Visual Evaluation of FLAIR Images

Results of the LST were compared with visual evaluation in three exemplary patients. Visual evaluation was performed by two neuroradiologists with long professional experience (S.G.: >30 years; W.C.: 8 years). The choice of patients included one patient evaluated with inconspicuous FLAIR images, one patient with unspecific FLAIR lesions, and one patient with ALS-specific FLAIR lesions in the pyramidal tracts (PT).

### Separate Control Analysis on T<sub>1</sub> Registration

A separate control analysis was conducted to investigate the effects of the preceding T<sub>1</sub> registration on LPA results. The healthy control group ( $n = 31$ ) and a subset of patients ( $n = 20$ ) were included in this control analysis. Control analysis in patients was restricted to a subgroup due to lack of T<sub>1</sub> data in eight patients. Threshold  $\kappa$  was set to 0.5 in both groups.

### Statistical Analysis

Two univariate analyses of variance (ANOVAs) (TLV, TLN) took into account factors group (ALS, controls), sex, and covariate age and investigated differences in TLV and TLN between all 28 ALS patients and all 31 healthy controls. ANOVA effects were analyzed by independent and dependent  $t$ -tests. Bravais–Pearson correlation analyses examined the relation of TLV and TLN to age, ALSFRS-R scores, disease progression rates, and elapsed time since diagnosis. Chi-square tests of independence were applied to analyze differences in frequencies of FLAIR lesions between ALS patients and healthy controls in most affected WM regions. Survival since diagnosis was analyzed by the Kaplan–Meier log-rank test. Seven out of 28 ALS patients were still alive and considered as censored data. In these seven patients, survival was calculated as the time span between diagnosis and MRI scan. Cox-regression analysis was used to investigate the effects of potential prognostic factors (age, sex, ALSFRS-R scores, disease progression rates) on survival. Separate control analysis examined the effects of precedent T<sub>1</sub> registration on LST results. This control analysis was performed using repeated-measures ANOVAs including a within-subject factor (with or without preceding T<sub>1</sub> registration), between-subject factors group (ALS, controls) and sex, and the covariate age for both TLV and TLN. The significance level was set to  $P < 0.05$ . Multiple comparison errors were controlled for by use of Bonferroni correction.

## Results

### Participants

In all, 28 ALS patients (eight females) were compared with 31 age-matched controls (12 females). The characteristics of ALS patients and healthy controls are summarized in Table 1. ALS patients did not significantly differ from healthy controls in age ( $T(57) = -1.560$ ;  $P = 0.124$ ). Sex-specific differences

in age were detected neither between ALS patients and healthy controls (females:  $T(18) = -0.826$ ,  $P = 0.420$ ; males:  $T(37) = -1.307$ ,  $P = 0.199$ ) nor within groups (ALS:  $T(26) = 0.268$ ,  $P = 0.792$ ; controls:  $T(29) = 0.076$ ,  $P = 0.940$ ).

### Total Lesion Number and Volume

Two univariate ANOVAs (ALS  $n = 28$ , healthy controls  $n = 31$ ) revealed highly significant effects of covariate age on both TLV ( $F(1,54) = 22.171$ ,  $P < 0.001$ ) and TLN ( $F(1,54) = 24.659$ ,  $P < 0.001$ ). These findings were supported by highly significant correlations of age with TLV ( $r = 0.529$ ,  $P < 0.001$ , corrected) and TLN ( $r = 0.554$ ,  $P < 0.001$ , corrected). TLN was significantly dependent on sex ( $F(1,54) = 5.720$ ,  $P = 0.020$ ) and tended to be higher in male compared with female participants ( $T(57) = 2.261$ ,  $P = 0.028$ , uncorrected). Age was not significantly different between male and female participants ( $T(57) = 0.374$ ,  $P = 0.711$ ). ALS patients showed a significant increase in TLN compared with healthy controls dependent on sex ( $F(1,54) = 5.076$ ,  $P = 0.028$ ) (Fig. 1a). FLAIR lesions were significantly more frequent in male ALS patients than in female ALS patients ( $T(26) = 3.879$ ,  $P < 0.001$ , corrected; males:  $n = 20$ ,  $M = 8.55$ ,  $SD = 5.978$ , females:  $n = 8$ ,  $M = 2.375$ ,  $SD = 2.44$ ) and tended to be more common than in male healthy controls ( $n = 19$ ) ( $T(37) = -2.020$ ,  $P = 0.051$ ). TLN did not significantly differ between female ALS patients and female healthy controls ( $n = 12$ ) ( $T(18) = 1.237$ ,  $P = 0.233$ ) or between female and male healthy controls ( $T(29) = 0.136$ ,  $P = 0.893$ ). No significant differences in age were observed between female and male ALS patients ( $T(26) = 0.268$ ,  $P = 0.792$ ), between male controls and male ALS patients ( $T(37) = -1.307$ ,  $P = 0.199$ ), or between female controls and female ALS patients ( $T(18) = -0.826$ ,  $P = 0.420$ ). The most pronounced levels of TLN were observed in two patients with bulbar-onset. TLV did not significantly differ between ALS patients and healthy controls ( $F(1,54) = 1.407$ ,  $P = 0.241$ ) or between sex

**TABLE 1. Characteristics of ALS Patients ( $n = 28$ ) and Age-Matched Healthy Controls ( $n = 31$ )**

	<i>n</i>	Mean age (yrs)	Median ALSFRS-R	Median disease progression rate	Time since diagnosis (months)
ALS	28	50.10 [24–73]	37.50 [21–48]	0.47 [0–4]	11 [1–43]
Controls	31	45.06 [25–67]			

ALS patients are described by median ALSFRS-R score, median disease progression rate ( $(48 - \text{ALSFRS-R}) / \text{months since symptom onset}$ ), and elapsed time between diagnosis and MRI scan (months).

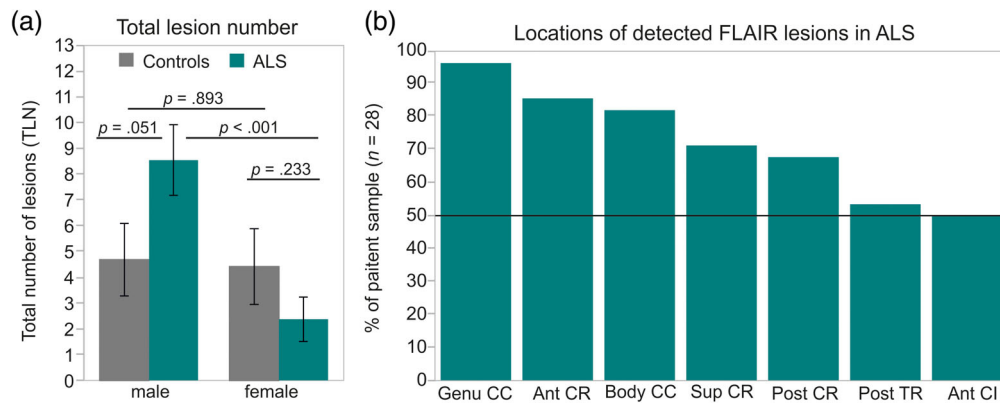


**FIGURE 1: Total lesion number and locations of FLAIR lesions detected by LPA. (a) TLN of healthy controls (gray, male:  $n = 19$ , female:  $n = 12$ ) and ALS patients (cyan, male:  $n = 20$ , female:  $n = 8$ ). (b) Percent of ALS patients showing FLAIR lesions in the most affected WM regions. Ant CR = anterior corona radiata; sup CR = superior corona radiata; post CR = posterior corona radiata; post TR = posterior thalamic radiation; ant CI = anterior capsula interna. P-values refer to two-sample t-tests.**

( $F(1,54) = 1.639, P = 0.206$ ). No significant interaction effect of sex with group (ALS, controls) was observed for TLV ( $F(1,54) = 1.562, P = 0.202$ ). TLN and TLV were strongly intercorrelated ( $r = 0.790, P < 0.001$ , corrected).

### Characteristics of FLAIR Lesions

Individual binary lesion maps of ALS patients ( $n = 28$ ) revealed most frequent FLAIR lesions in the callosal genu ( $n = 27$ ) and body ( $n = 23$ ), the anterior ( $n = 24$ ), superior ( $n = 20$ ), and posterior ( $n = 19$ ) corona radiata, posterior thalamic radiation ( $n = 15$ ), and the anterior capsula interna ( $n = 14$ ) (Fig. 1b). Healthy controls ( $n = 31$ ) exhibited similar frequency of FLAIR alterations in the genu ( $\chi^2(1) = 0.253, P = 0.615, \phi = 0.065$ ), body ( $\chi^2(1) = 1.015, P = 0.314, \phi = 0.131$ ) and the anterior corona radiata ( $\chi^2(1) = 0.024, P = 0.877, \phi = 0.020$ ). However, FLAIR lesions in the superior ( $\chi^2(1) = 6.345, P = 0.012, \phi = 0.328$ ) and posterior corona radiata ( $\chi^2(1) = 7.460, P = 0.006, \phi = 0.356$ ), posterior thalamic radiation ( $\chi^2(1) = 6.042, P = 0.014, \phi = 0.320$ ), and marginally in the anterior capsula interna ( $\chi^2(1) = 3.683, P = 0.055, \phi = 0.250$ ) were significantly more frequent in ALS patients than in healthy controls.

FLAIR lesions at the ventricular borders were detected in ALS patients as well as in healthy controls. Individual binary lesion maps across all ALS patients were accumulated into an overlap lesion map (Fig. 2). FLAIR lesions of ALS patients were small (TLV:  $M = 0.72$  ml,  $SD = 0.22$ ) and diffuse. 65% of voxels with FLAIR alterations showed no overlap between ALS patients.

### Quantitative and Subjective Evaluation of FLAIR Images

The results of LST were compared with visual evaluation of FLAIR images by two experienced neuroradiologists (Fig. 3). Both neuroradiologists classified the FLAIR images of patient 1 (Fig. 3a) as age-related without abnormalities. LST only marked regions at the ventricular border. Patient 2 (Fig. 3b) was evaluated with multiple small and unspecific WM lesions but weak to no evidence for pathological signal change in PTs. Consistent with this visual evaluation, LST detected no lesions in PTs but the presence of unspecific WM lesions (white arrow, Fig. 3b). Patient 3 (Fig. 3c) was evaluated with symmetrical signal change along the PTs in both LST and visual evaluation of the two neuroradiologists. Increased FLAIR signal in the PTs was not evaluated as an artifact, as it

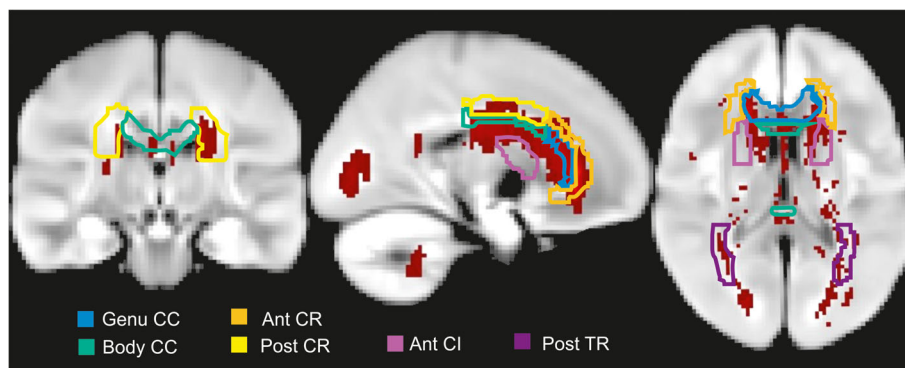


**FIGURE 2: Localization and distribution of FLAIR lesions in ALS patients. Overlap of individual binary lesion maps summed up across all ALS patients ( $n = 28$ ). CC = corpus callosum; Ant CR = anterior corona radiata; post CR = posterior corona radiata; post TR = posterior thalamic radiation; ant CI = anterior capsula interna.**

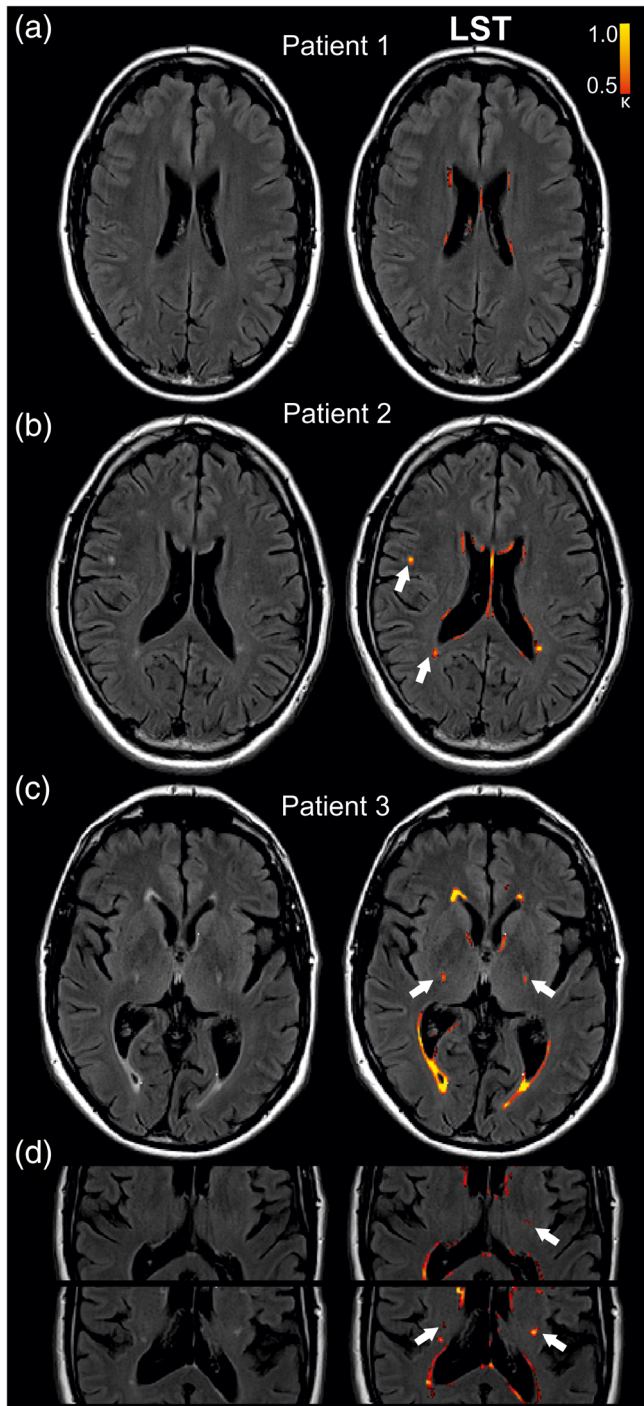


**FIGURE 3:** Lesion segmentation in three exemplary patients. MRI slices of three limb-onset patients (Patient 1: 46-year-old, male, ALSFRS-R: 39; Patient 2: 46-year-old, male, ALSFRS-R: 48, Patient 3: 69-year-old, male, ALSFRS-R: 21) FLAIR images were evaluated by two experienced neuroradiologists and LST (red). (a) Patient 1 evaluated with age-related FLAIR images. (b) Slice of FLAIR images of Patient 2 described by unspecific WM lesions and weak to no evidence for pathological signal change in the PTs. LST successfully detected unspecific WM lesions (white arrows). (c) Evaluation of symmetric hyperintensity signal in the PTs of Patient 3 by both LST and visual evaluation of two neuroradiologists. (d) Persistent hyperintensity in the PT across the following MRI slices of Patient 3. Threshold for lesion probability was  $\kappa = 0.50$ . PT = pyramidal tract.

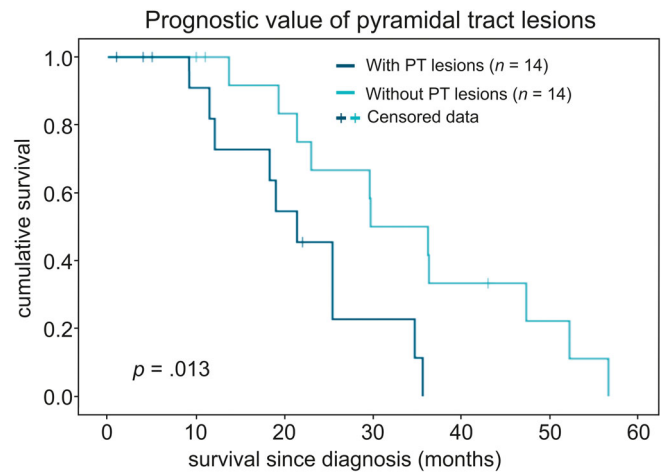


**FIGURE 4:** Prognostic value of PT lesions for survival since diagnosis. PT lesions were detected by the LST in 14 out of 28 patients. Kaplan–Meier analysis revealed significantly inferior survival prognosis for patients with PT lesions (dark cyan) compared with those without PT lesions (bright cyan) ( $P = 0.013$ ). Seven out of 28 patients were still participating in the study and were marked as censored data.

was persistent across the following brain slices (Fig. 3d). Signal changes along the PTs as visualized in Patient 3 were marked by LST in 14 out of 28 ALS patients.

### Clinical Correlations

LST variables did not significantly correlate with disease progression rates (TLV:  $r = 0.045$ ,  $P = 0.820$ ; TLN:  $r = -0.101$ ,  $P = 0.608$ ). ALSFRS-R scores at baseline significantly correlated with elapsed time between diagnosis and MRI scan ( $r = -0.520$ ,  $P = 0.005$ , corrected). However, ALSFRS-R sum scores only weakly correlated with TLV of ALS patients ( $r = -0.417$ ,  $P = 0.027$ , uncorrected) and showed no significant correlation with survival since diagnosis ( $r = 0.136$ ,  $P = 0.569$ ). A tendency towards an association between TLN and survival ( $r = -0.445$ ,  $P = 0.050$ , uncorrected) led to the following post-hoc analysis: Patients were differentiated into patients with ( $n = 14$ ) or without ( $n = 14$ ) PT lesions as detected by the LST. Overall estimated mean survival time was 29.08 months since diagnosis (95% confidence interval [CI] 23.31–34.85 months). Kaplan–Meier log-rank test revealed significantly inferior survival since diagnosis for patients with PT lesions (95% CI 16.5–27.7 months) compared with those without PT lesions (95%CI 26.51–43.04 months) ( $P = 0.013$ ) (Fig. 4). Cox-regression analysis demonstrated the prognostic value of age (hazard ratio: 1.067, CI: 1.01–1.12;  $P = 0.015$ ) for survival. No prognostic value was observed for ALSFRS-R scores ( $P = 0.964$ ), disease progression rates ( $P = 0.154$ ) or sex ( $P = 0.245$ ).

### Control Analysis on Preceding T<sub>1</sub> Registration

A separate control analysis (ALS  $n = 20$ , controls  $n = 31$ ) investigated bias effects of precedent T<sub>1</sub> registration on LPA

lesion segmentation. Registration to  $T_1$  images did not significantly affect TLN ( $F(1,46) = 0.008$ ,  $P = 0.930$ ). In contrast, TLV was significantly increased if LPA was preceded by registration of FLAIR images to  $T_1$  images ( $F(1,46) = 7.538$ ,  $P = 0.009$ ).

## Discussion

LST revealed enhanced frequency of FLAIR alterations in male ALS patients. FLAIR lesions were small and diffuse and more frequent in ALS patients than in healthy controls in the superior and posterior corona radiata, posterior thalamic radiation, and anterior capsula interna. The presence of PT lesions as detected by the LST was associated with inferior survival.

FLAIR lesions may be interpreted as loss of myelination in fibers.<sup>17</sup> In healthy subjects, FLAIR alterations were observed to increase with age.<sup>7</sup> Consistent with this finding, we detected distinct effects of age on TLN and TLV. LST revealed FLAIR hyperintensity in both ALS patients and healthy controls, as reported in other studies.<sup>8,13,14,23</sup> FLAIR lesions were observed to be dependent on sex and more frequent in male ALS patients than in female ALS patients as well as male healthy controls. In contrast, healthy controls showed no sex-specific differences in FLAIR alterations, as reported by Gawne-Cain et al.<sup>7</sup> Sex-specific differences in FLAIR lesions were reported for MS patients despite balanced age and disease duration.<sup>24</sup> In ALS research, effects of sex on FLAIR hyperintensity were not detected<sup>23</sup> or not analyzed.<sup>8,10,12,14,16,25,26</sup> Sex-specific differences may be due to outliers with low TLN in the small sample size of female ALS patients ( $n = 8$ ). Consistent with this consideration, several studies failed to detect FLAIR alterations in all ALS patients of the sample.<sup>13,16,25,27,28</sup> FLAIR alterations were discussed to occur predominantly in patients with a progressed stage of ALS.<sup>13,25,29</sup> The two patients with the highest TLN had bulbar-onset of disease. This finding is consistent with Vazques-Costa et al.<sup>23</sup> reporting more pronounced FLAIR signal change of the CST in bulbar- compared with limb-onset patients. Total lesion volumes in ALS patients were comparable to that of healthy controls and much lower than in other neurological diseases such as MS.<sup>21</sup> These findings are consistent with previous studies reporting the dominant role of frequency rather than volumes of FLAIR alterations in ALS.<sup>13,14</sup>

FLAIR lesions in ALS patients were most prominent in the corona radiata and body and genu of the CC. These findings are consistent with a study<sup>12</sup> reporting most pronounced FLAIR hyperintensity of classic ALS in corona radiata of the CST and the body of the CC. Similarly, we observed FLAIR lesions to be more frequent in ALS patients than in healthy controls in the superior and posterior corona radiata. FLAIR alterations in the CC were shared in both ALS patients and healthy controls. These findings may indicate that detected callosal FLAIR lesions may be age-related<sup>7</sup> or may result from

FLAIR artifacts.<sup>30</sup> Moreover, FLAIR alterations were detected at the ventricular borders. FLAIR hyperintensity visualized as thin lines surrounding ventricles is a frequently observed phenomenon also in healthy controls<sup>7</sup> and may be associated with cerebrospinal fluid/vascular pulsation artifacts<sup>30</sup> or artifacts originating from incomplete signal inversion.<sup>31</sup> However, structural changes at the ventricular borders may as well indicate processes in the region of neurogenesis (subventricular zone).<sup>32</sup> LST detected FLAIR alterations at the PT in 14 out of 28 patients. These lesions often appeared to be symmetric across hemispheres as reported in Cheung et al.<sup>33</sup> The good correspondence of LST results to findings of visual evaluation<sup>8,10,13,24</sup> and quantitative evaluation<sup>8,10,12</sup> argue for the potential of LST use. The interpretation of numerical TLN and TLV should be done carefully, as LST may be biased by hyperintensity derived from incomplete signal inversion along the ventricular walls resulting in CSF-ventricular-border-artifacts. Still, LST was useful in the fast and objective detection of intracerebral lesions.

Correlations of both ALSFRS-R and disease progression rates with LST variables were rather weak or not detectable. Lack of correlation between FLAIR intensity and clinical data was frequently reported in both visual evaluation studies<sup>9,11,34</sup> and quantitative studies.<sup>8,16</sup> Kaplan–Meier analysis detected inferior survival for patients with PT lesions compared with patients without PT lesions. Thus, the LST may not only help to monitor intracerebral lesions but may also contribute to prognosis and diagnosis of different ALS phenotypes. Cox-regression analysis revealed significant prognostic value of age for survival. This is consistent with Pupillo et al.<sup>35</sup> showing age as one of the most relevant prognostic factors of ALS survival. The baseline ALSFRS-R score significantly correlated with elapsed time between diagnosis and MRI scan, but had no predictive value for the survival of patients. Prognostic values of sex, ALSFRS-R scores, and disease progression rates on survival were less consistently reported than that of age.<sup>36</sup>

Several methodological limitations may be considered. First, the sample size was limited to  $n = 28$  patients. The subset of female patients did not show severe FLAIR lesions potentially affecting group statistics. Still, the sample size was adequate to detect a higher frequency of FLAIR lesions in male patients at the group level. Second, the sample included both limb-onset and bulbar-onset patients. Lack of balanced sample sizes (limb-onset:  $n = 25$ , bulbar-onset:  $n = 3$ ) allowed for no statistical test for ALS onset. A separate control analysis revealed that TLV was biased by precedent  $T_1$  registration. TLN was stable in  $T_1$  registration. Thus, precedent registration of lower-resolution FLAIR data to higher-resolution  $T_1$  images may bias the size of detected FLAIR lesions.

In conclusion, LST is an accessible and time-saving tool for objective quantification of FLAIR alterations in ALS. The predictive value of FLAIR alterations for survival prognosis underlines the relevance of monitoring FLAIR images in ALS

patients and its potential for the classification of ALS phenotypes. Future studies may explore FLAIR alterations detected by LST in different ALS subtypes and ALS mimic disorders to underline ALS-specificity of these FLAIR lesions.

## Contributions

Anna Maria Wirth: conception and design of the study, acquisition, analysis, interpretation of MRI data, and composition of the article. Siw Johannesen, Tim-Henrik Bruun, Ulrich Bogdahn: contribution to the conception of the study; acquisition, analysis, and interpretation of clinical data, and revision of the article. Andrei Khomenko, Dobri Baldaranov: data acquisition and revision of the article. Siw Johannesen, Andrei Khomenko, Dobri Baldaranov, Ulrich Bogdahn: care for ALS patients in outpatient clinic, treatment concept. Gerhard Schuierer, Christina Wendl: MRI data acquisition and visual evaluation of MRI data. Mark William Greenlee: contribution to the conception of the study, supervision of MRI data analysis and data interpretation, and revision of the article. All authors appropriately accounted for the accuracy and integrity of the current project.

## Conflict of Interest

The authors declare no commercial or financial conflicts of interest.

## References

- Al-Chalabi A, Hardiman O, Kiernan MC, Chiò A, Rix-Brooks B, van den Berg LH. Amyotrophic lateral sclerosis: moving towards a new classification system. *Lancet Neurol* 2016;15:1182–1194.
- Tao QQ, Wu ZY. Amyotrophic lateral sclerosis: Precise diagnosis and individualized treatment. *Chin Med J (Engl)* 2017;130:2269–2272.
- Bede P, Querin G, Pradat P-F. The changing landscape of motor neuron disease imaging: The transition from descriptive studies to precision clinical tools. *Curr Opin Neurol* 2018;31:431–438.
- Cohen-Ahad J, Mendili M-M, Morizot-Koutlidis R, et al. Involvement of spinal sensory pathway in ALS and specificity of cord atrophy to lower motor neuron degeneration. *Amyotroph Lateral Scler Frontotemporal Degener* 2013;14:30–38.
- Gramsch C, Nensa O, Kastrup S, et al. Diagnostic value of 3D fluid attenuated inversion recovery sequence in multiple sclerosis. *Acta Radiol* 2015;56:622–627.
- Hajnal JV, Bryant DJ, Kasuboski L, et al. Use of fluid attenuated inversion recovery (FLAIR) pulse sequences in MRI of the brain. *J Comput Assist Tomogr* 1992;1:841–844.
- Gawne-Cain ML, Silver NC, Moseley IF, Miller DH. Fast FLAIR of the brain: The range of appearances in normal subjects and its application to quantification of white-matter disease. *Neuroradiology* 1997;39:243–249.
- Hecht MJ, Fellner F, Hilz MJ, Heuss D, Neundorfer B. MRI-FLAIR images of the head show corticospinal tract alterations in ALS patients more frequently than T2-, T1-, and proton-density-weighted images. *J Neurol Sci* 2001;186:37–44.
- Gupta A, Nguyen TB, Chakraborty S, Bourque PR. Accuracy of conventional MRI in ALS. *Can J Neurol Sci* 2014;41:53–57.
- Schweitzer AD, Liu T, Gupta A, et al. Quantitative susceptibility mapping of the motor cortex in amyotrophic lateral sclerosis and primary lateral sclerosis. *Am J Roentgenol* 2015;204:1086–1092.
- Jin J, Hu F, Zhang Q, Jia R, Dang J. Hyperintensity of the corticospinal tract on FLAIR: A simple and sensitive objective upper motor neuron degeneration marker in clinically verified amyotrophic lateral sclerosis. *J Neurol Sci* 2016;367:177–183.
- Fabes J, Matthews L, Fillippini N, Talbot K, Jenkinson M, Turner MR. Quantitative FLAIR MRI in amyotrophic lateral sclerosis. *Acad Radiol* 2017;24:1187–1194.
- Thorpe JW, Moseley IF, Hawkes C, MacManus DG, McDonald WI, Miller DH. Brain and spinal cord MRI in motor neuron disease. *J Neurol Neurosurg Psychiatry* 1996;61:314–317.
- Zhang L, Ulug AM, Zimmerman RD, Lin MT, Rubin M, Beal MF. The diagnostic utility of FLAIR imaging in clinically verified amyotrophic lateral sclerosis. *J Magn Reson Imaging* 2003;17:521–527.
- Protogerou G, Ralli S, Tsougos I, et al. T2 FLAIR increased signal intensity at the posterior limb of the internal capsule: Clinical significance in ALS patients. *Neuroradiol J* 2011;24:226–234.
- Hecht MJ, Fellner F, Fellner C, Hilz MJ, Heuss D, Neundorfer B. Hyperintense and hypointense MRI signals of the precentral gyrus and corticospinal tract in ALS: a follow-up examination including FLAIR images. *J Neurol Sci* 2002;199:59–65.
- Schmidt P, Gaser C, Arsic M, et al. An automated tool for detection of FLAIR-hyperintense white-matter lesions in multiple sclerosis. *Neuroimage* 2012;59:3774–3783.
- World Medical Association. World Medical Association Declaration of Helsinki: Ethical principles for medical research involving human subjects. *JAMA* 2013;310:20.
- Winkler AM, Kochunov P, Glahn DC. FLAIR templates. Available at <http://brainder.org>
- Schmidt P. Bayesian inference for structured additive regression models for large-scale problems with applications to medical imaging. <http://nbn-resolving.de/urn:nbn:de:vbv:19-203731> (2017).
- Egger C, Opfer R, Wang C, et al. MRI FLAIR lesion segmentation in multiple sclerosis: Does automated segmentation hold up with manual annotation? *NeuroImage Clin* 2016;13:264–270.
- Mori S, Oishi K, Jiang H, et al. Stereotaxic white matter atlas based on diffusion tensor imaging in an ICBM template. *NeuroImage* 2008;40:570–582.
- Vazquez-Costa JF, Mazon M, Carreres-Polo J, et al. Brain signal intensity changes as biomarkers in amyotrophic lateral sclerosis. *Acta Neurol Scand* 2018 <https://doi.org/10.1111/ane.12863>.
- Klistorner A, Wang C, Yiannikas C, Graham SL, Parratt J, Barnett MH. Progressive injury in chronic multiple sclerosis lesions is gender-specific: A DTI study. *PLoS One* 2016;11:e0149245.
- Ignjatovic A, Stevic Z, Lavrnjic S, Dakovic M, Bacic G. Brain iron MRI: A biomarker for amyotrophic lateral sclerosis. *J Magn Reson Imaging* 2013;38:1472–1479.
- Ngai S, Tang YM, Du L, Stuckey S. Hyperintensity of the precentral gyral subcortical white matter and hypointensity of the precentral gyrus on fluid-attenuated inversion recovery: Variation with age and implications for the diagnosis of amyotrophic lateral sclerosis. *AJNR Am J Neuroradiol* 2007;28:250–254.
- Ishikawa K, Nagura H, Yokota T, Yamaouchi H. Signal loss in the motor cortex on magnetic resonance images in amyotrophic lateral sclerosis. *Ann Neurol* 1993;33:218–222.
- da Rocha AJ, Oliveira AS, Fonseca RB, Maia AC, Buainain RP Jr, Lederman HM. Detection of corticospinal tract compromise in amyotrophic lateral sclerosis with brain MR imaging: Relevance of the T1-weighted spin-echo magnetization transfer contrast sequence. *AJNR Am J Neuroradiol* 2004;25:1509–1515.
- Huynh W, Simon NG, Grosskreutz J, Turner MR, Vucic S, Kiernan MC. Assessment of the upper motor neuron in amyotrophic lateral sclerosis. *Clin Neurophysiol* 2016;127:2643–2660.
- Krupa K, Bekiesińska-Figatowska M. Artifacts in magnetic resonance imaging. *Pol J Radiol* 2015;80:93–106.

31. Hajnal JV, Oatridge A, Herlihy AH, Bydder GM. Reduction of CSF artifacts on FLAIR images by using adiabatic inversion pulses. *AJNR* 2001; 22:317–322.
32. Bergmann O, Spalding KL, Frisén J. Adult neurogenesis in humans. *Cold Spring Harb Perspect Biol* 2015;7:a018994.
33. Cheung G, Gawel MJ, Cooper PW, Farb RI, Ang LC, Gawal MJ. Amyotrophic lateral sclerosis: Correlation of clinical and MR imaging findings. *Radiology* 1995;194:263–270.
34. Peretti-Viton P, Azulay JP, Trefouret S, et al. MRI of the intracranial corticospinal tracts in amyotrophic and primary lateral sclerosis. *Neuroradiology* 1999;41:744–749.
35. Pupillo E, Messina P, Logroscino G, et al. Long-term survival in amyotrophic lateral sclerosis: A population-based study. *Ann Neurol* 2014;75: 287–297.
36. Chiò A, Logroscino G, Hardiman O, et al. Prognostic factors in ALS: A critical review. *Amyotrophic Lateral Sclerosis* 2009;10:310–323.